analytical chemistry

Article

pubs.acs.org/ac

Near-Infrared Fluorescent Probe for Imaging Mitochondrial Hydrogen Polysulfides in Living Cells and in Vivo

Min Gao,[†,‡] Fabiao Yu,[†] Hao Chen,[†] and Lingxin Chen*[,†,‡]

[†]Key Laboratory of Coastal Environmental Processes and Ecological Remediation, The Research Center for Coastal Environmental Engineering and Technology, Yantai Institute of Coastal Zone Research, Chinese Academy of Sciences, Yantai 264003, China

[‡]The Key Laboratory of Life-Organic Analysis, College of Chemistry and Chemical Engineering, Qufu Normal University, Qufu 273165, China

Supporting Information

ABSTRACT: Hydrogen polysulfides (H_2S_n, $n > 1$), derived from hydrogen sulfide (H_2S), have attracted increasing attention in biochemical research, which may perform as the actual signaling molecules during cell signaling processes. Because of the closed biological and chemical relationship between H_2S and H_2S_n, it is of great value to develop sensitive and specific techniques to distinguish the intracellular level of H_2S_n. To improve the understanding of the physiological and pathological roles played by H_2S_n, we now develop a specific fluorescent probe Mito-ss for capturing H_2S_n in cells and in vivo. When triggered by H_2S_n, Mito-ss replies a turn-on fluorescence signal and exhibits a higher selectivity toward H_2S_n than other abundant competing biothiols, such as glutathione, cysteine and H_2S. The probe Mito-ss can also be applied to visual H_2S_n in living cells, as well as in vivo, providing a potentially powerful approach for probing H_2S_n in biological systems.

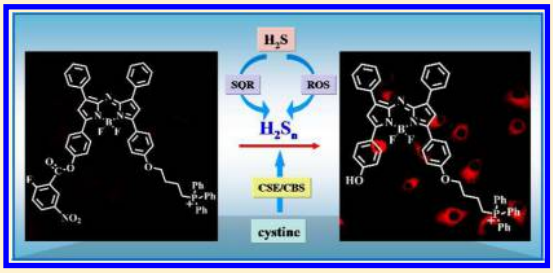

Reactive sulfur species (RSS) which belong to sulfur-containing molecules touch on every aspects of cellular biology and regulate oxidative stress and redox signaling.[1−4] In general, these molecules include glutathione (GSH), cysteine (Cys), hydrogen sulfide (H_2S), persulfides, polysulfides, and S-modified cysteine adducts, such as *S*-nitrosothiols and sulfenic acids. Among them, H_2S exerts regulative function of intracellular redox status and connects with various physiological and pathological processes, which has been considered as the endogenous signaling molecular.[5−7] However, many of the underlying biological mechanisms are still unclear. As is known, H_2S is often considered to be a mitochondrial poison. A high concentration of exogenously added H_2S can be controlled through consumption by mitochondrial enzyme sulfide quinone reductase (SQR) and converted into the polysulfur species (persulfides and polysulfides) pool rapidly, which exhibit low toxicity in biological systems. They are mainly stored in the mitochondria until released in response to physiologic signals.[8] As the direct redox form of H_2S, hydrogen polysulfides (H_2S_n, $n > 1$), a combination of polysulfur molecules, behave the properties of antioxidant, cytoprotection, and redox signaling. H_2S_n modulate many cellular functions through an array of intracellular redox signaling processes by mercapto (−SH) modification.[9−11] In addition, more and more studies imply that biological activities associated with H_2S may actually be mediated by or based on H_2S_n.[12−15] For example, H_2S_n can induce Ca^{2+} influx by activating transient receptor potential (TRP) A1 channels in astrocytes, which previously has been attributed to the activity of H_2S.[16] Therefore, it is reasonable to infer that H_2S_n may be the actual signaling species, while H_2S may only play a role as a marker for the biologically active of H_2S_n species.

To obtain more information about the chemical and biological properties of H_2S_n, an accurate and sensitive method for detecting H_2S_n in biosystems is urgently required. However, the rapid catabolism of H_2S_n will result in the continuous fluctuation of its concentration. It is also impossible to separate H_2S_n from biological systems immediately. All these issues make it difficult to detect H_2S_n accurately. The traditional detection method for H_2S_n is by measuring UV absorption peaks at 290−300 and 370 nm.[17] However, this method requires sample processing, which will destruct the tissues or cell lysates, so it is not suitable for fast, accurate, and real-time determination of biological samples. Fluorescence-based assays with its real-time detection and convenience, in particularly, offer the potentiality to tackle this unmet need by mapping the spatial and temporal distribution of H_2S_n in living cells.[18−30] To date, only Xian's group reported two series of fluorescent probe with short emission wavelength for selective detection of exogenous H_2S_n in living cells.[31,32] As known, near-infrared (NIR) light can penetrate tissue more deeply and minimize the interference from background autofluorescence, which greatly facilitates in vivo imaging of molecular processes. Herein, we present the design, synthesis, and application of a NIR

Received: September 19, 2014
Accepted: March 9, 2015
Published: March 9, 2015

DOI: 10.1021/ac5044237
Anal. Chem. 2015, 87, 3631−3638

Scheme 1. Synthesis Route for Mito-ss

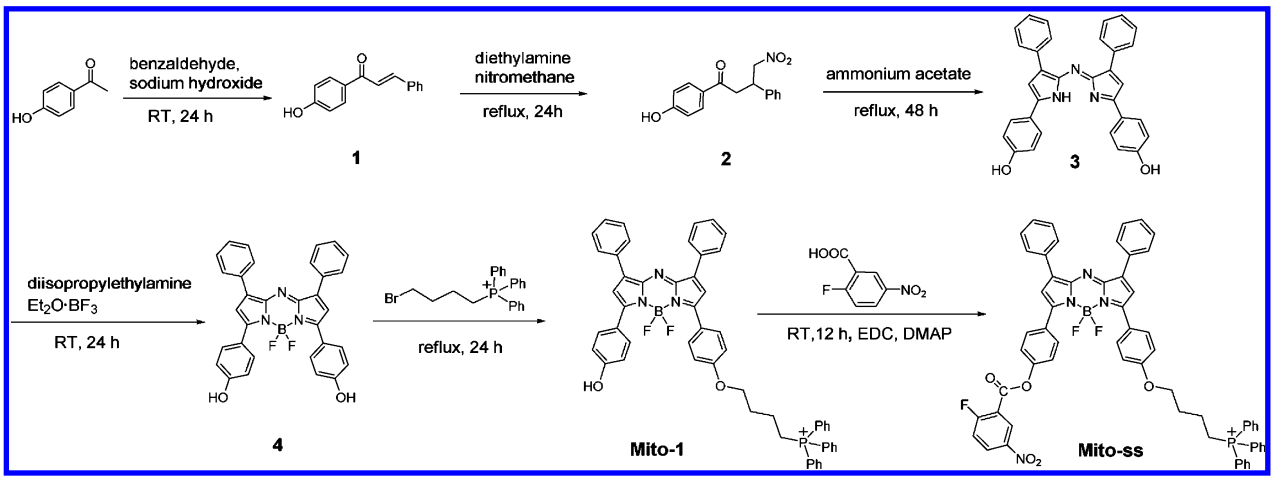

fluorescent probe, Mito-ss, which possesses enhanced sensitivity and cellular trappability to H_2S_n. This mitochondria-targeted probe is also available for real-time imaging endogenous H_2S_n produced in living RAW264.7 cells, as well as in mice.

■ EXPERIMENTAL SECTION

Reagents and Apparatus. All chemicals used in synthesis are analytical reagent grade, and were used as received. Ultrapure water was used throughout. Thin-layer chromatography (TCL) was performed on silica gel plates. Silica gel P60 (SiliCycle) was used for column chromatography (Hailang, Yantai) 200−300 mesh. Absorption spectra were collected on a Thermo Scientific NanoDrop 2000/2000C spectrophotometer. Fluorescence spectra were determined using a HORIBA Scientific Fluoromax-4 spectrofluorometer. All pH measurements were performed with a basic pH-Meter PH-3C digital pH-meter (Lei Ci Device Works, Shanghai) with a combined glass-calomel electrode. ^{1}H NMR and ^{13}C NMR spectra were recorded employing a Bruker AVANCE IIITM 500 spectrometer. Fluorescent images of cells were acquired on an Olympus FluoView FV1000 laser-scanning microscope with an objective lens (×40). Compounds were efficiently synthesized following the synthetic methodology shown in Scheme 1.

Synthesis of Mito-1. The synthetic procedure of compounds **1**−**4** were performed in the Supporting Information. A solution of compound **4** (52.9 mg, 0.1 mmol) in acetone (50 mL) was treated with K_2CO_3 (28.8 mg, 0.21 mmol); then (4-bromobutyl)triphenylphosphonium bromide (47.8 mg, 0.1 mmol) was dropwised into the mixture over a period of 30 min.[33] The mixture was heated under reflux for 24 h. Then the mixture was neutralized with dilute HBr, partitioned between CH_2Cl_2 (50 mL) and H_2O (50 mL). The organic layer was separated and evaporated under reduced pressure. Purification by column chromatography on silica eluting with EtOAc/CH_3OH (3:1, v/v) gave the product (Mito-1) as a green solid. Yield: 35 mg, 37.8%. ^{1}H NMR (500 MHz, $CDCl_3$-D_1): δ (ppm): 9.59 (s, 1H), 8.06−8.02 (m, 2H), 7.97−7.92 (m, 4H), 7.87−7.81 (m, 5H), 7.79−7.71 (m, 2H), 7.70−7.58 (m, 16H), 7.18−7.16 (d, 2H), 7.05 (s, 1H), 6.79 (s, 1H), 6.64−6.62 (d, 2H), 4.14−4.10 (t, 2H), 1.75−1.73 (m, 2H), 0.97−0.92 (m, 4H). ^{13}C NMR (125 MHz, $CDCl_3$-D_1) δ (ppm): 172.16, 171.15, 150.00, 147.83, 135.21, 133.79, 133.71, 133.52, 133.44, 130.62, 130.52, 129.27, 129.08, 128.55, 128.45, 118.97, 118.01, 117.48, 116.65, 114.47, 60.39, 29.70, 21.05, 14.20. LC-MS (ESI$^+$): m/z $C_{54}H_{44}BF_2N_3O_2P^+$ calcd. 846.3227, found [M$^+$] 846.3227.

Synthesis of Compound Mito-ss. A mixture of Mito-1 (92.6 mg, 0.1 mmol), 2-fluoro-5-nitrobenzoic acid (18.5 mg, 0.1 mmol), 1-(3-(dimethylamino)propyl)-3-ethylcarbodiimide hydrochloride (EDC, 19.2 mg, 0.1 mmol), and 4-dimethylaminopyridine (DMAP, 1.22 mg, 0.01 mmol) in CH_2Cl_2 (50 mL) was stirred for 12 h at room temperature.[34] Then the mixture was neutralized with dilute HBr, and partitioned between CH_2Cl_2 (50 mL) and H_2O (50 mL). Then solvent was evaporated under reduced pressure and resulted residue was subjected to column chromatography for purification (CH_2Cl_2). Probe Mito-ss was obtained as a green solid. Yield: 0.04 g, 36.6%. ^{1}H NMR (500 MHz, $CDCl_3$-D_1) δ (ppm): 8.95−8.90 (m, 1H), 8.4 6−8.41 (m, 1H), 8.00−7.96 (m, 5H), 7.75−7.65 (m, 27H), 7.02 (s, 1H), 6.90 (s, 1H), 6.83−6.81 (d, 2H), 4.10−4.08 (d, 2H), 1.80−1.75 (m, 2H), 0.81−0.79 (m, 4H). ^{13}C NMR (125 MHz, $CDCl_3$-D_1) δ(ppm): 165.48, 163.30, 160.80, 159.92, 159.23, 153.97, 150.46, 145.48, 143.97, 143.39, 142.97, 134.04, 134.01, 132.59, 131.56, 130.88, 129.51, 129.41, 128.75, 128.40, 128.20, 127.59, 127.51, 120.45, 117.95, 117.76, 117.53, 116.85, 113.91, 65.61, 28.67, 28.29, 26.19, 21.66, 20.63. LC-MS (ESI$^+$): m/z $C_{61}H_{46}BF_3N_4O_5P^+$ calcd. 1013.3245, found [M$^+$] 1013.3245.

■ RESULTS AND DISCUSSION

Probe Design and Synthesis. Because H_2S_n had two free −SH groups, we envisioned that H_2S_n would perform as a reactive nucleophile in biological systems that could participate in bis-nucleophilic substitution. Benefited from this chemical reaction, we expected that a well-conceived probe containing bis-electrophilc groups should be more efficient to capture H_2S_n. As an overall strategy, we chose the azo-BODIPY as fluorophore, which exhibited high molar absorption coefficient and NIR emission. Considering the electron-withdrawing group was often thought to be a strong quencher for fluorophore, we anticipated that the fluorescence properties of azo-BODIPY fluorophore could be manipulated through a photoinduced electron transfer (PET) process from the excited fluorophore to a strong electron-withdrawing group (donor-excited PET; d-PET).[35−37] After being fixed the fluorescence modulation mechanism, we selected a nitro-activated fluorobenzoiate as the d-PET modulator because it contained bis-electrophilc center

DOI: 10.1021/ac5044237
Anal. Chem. 2015, 87, 3631−3638

Scheme 2. Design Approach for Mito-ss

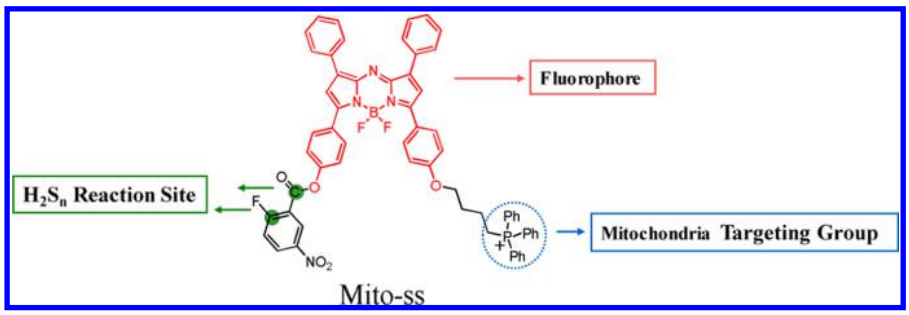

Scheme 3. Proposed Detection Mechanism of Mito-ss against H_2S_2/Biothiols

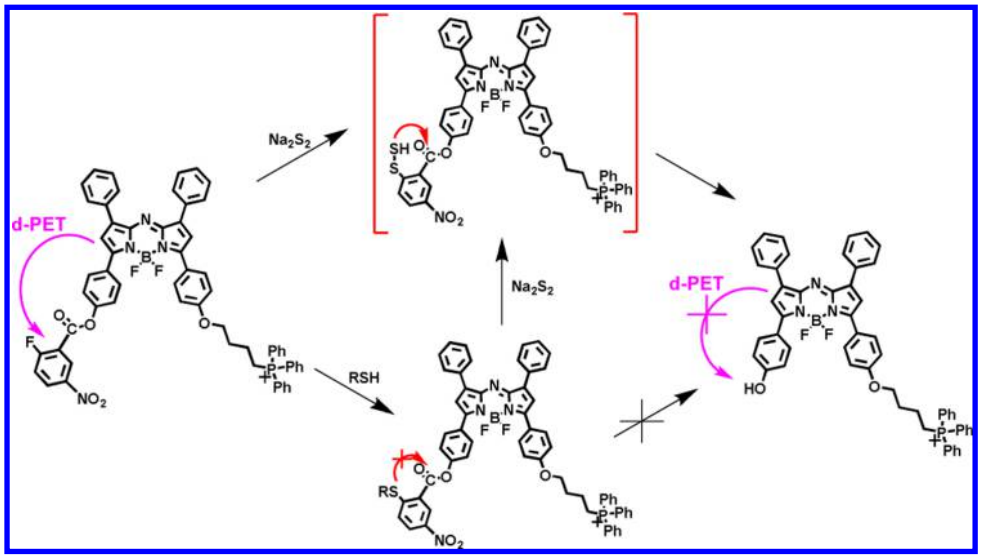

that could respond to H_2S_n selectively and sensitively. The azo-BODIPY fluorophore was first decorated with lipophilic triphenylphosphonium cation which enables the probe to have mitochondrial sublocation function in cells. After being modified with nitro-activated fluorobenzoiate into the azo-BODIPY platform, the fluorescence of the fluorophore was well quenched due to the d-PET process between the modulator and fluorophore. And finally, the well assembled probe was ready to work (Scheme 2).

Detection Mechanism. There exists a rapid dynamic equilibrium among H_2S_n species under certain pH condition.[16] In this paper, hydrogen disulfide (H_2S_2) was selected as a typical delegate of H_2S_n, because H_2S_2 could undergo the bis-electrophilc reaction more clearly. The proposed reaction mechanism was illustrated in Scheme 3. H_2S_2 should begin nucleophilic aromatic substitution (S_NAr) via replace F atom to form an intermediate containing free −SH group. Subsequently, the free −SH group continued a spontaneous intramolecular cyclization with the ester group to release the azo-BODIPY fluorophore. This tandem reaction would hinder the d-PET process timely, and therefore the fluorescence intensity increased significantly. More importantly, other monosubstituted thiols, such as Cys and GSH, could only proceed nucleophilic substitution once. The reaction of Mito-ss with biothiol *N*-acetyl-L-cysteine methyl ester demonstrated that no further cyclization product was isolated (see the Supporting Information). These results confirm that our hypothesis that certain bis-electrophilc groups can be used for capturing H_2S_n selectively.

Reaction Kinetics. With the promising probe in hand, we first evaluated Mito-ss (10 μM) toward Na_2S_2 (a common H_2S_2 donor, 10 μM) under simulated physiological conditions (10 mM HEPES buffer, pH 7.4). As expected, Mito-ss showed almost no fluorescence, whereas a fast and robust increase of the fluorescence intensity was obtained upon treatment with Na_2S_2 at 25 s (Figure 1). The results indicate that H_2S_2 can react with Mito-ss and induce the cleavage of ester group to release the fluorophore. Thereby, the fluorescence emission was "switched on", which was attributed to the removal of d-PET process. In addition, we found that Mito-ss displayed a very quick response to H_2S_2. Within a 30 s reaction time, the probe

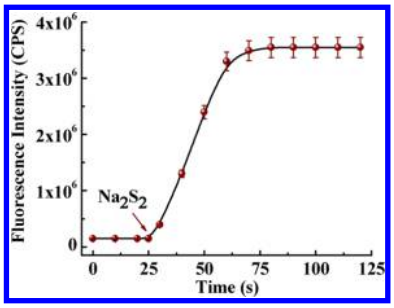

Figure 1. Time-dependent fluorescence intensity changes of Mito-ss (10 μM) toward Na_2S_2 (10 μM). Na_2S_2 was added at the reaction time of 25 s in 10 mM HEPES buffer (pH 7.4, 0.5% DMSO, 0.4% Tween 80). The reactions were measured during 120 s at 37 °C. λ_{ex} = 675 nm, λ_{em} = 730 nm.

DOI: 10.1021/ac5044237
Anal. Chem. 2015, 87, 3631−3638

offered a 24-fold turn-on emission. In view of the variable nature and rapid metabolism of endogenous H_2S_n in biological systems, the quick response behavior endows our probe a unique capability for real-time bioimaging of intracellular H_2S_2.

Spectroscopic Properties. The fluorescence responses of probe to H_2S_2 were also characterized over adding a range of concentrations of Na_2S_2 (Figure 2a). Upon treatment with

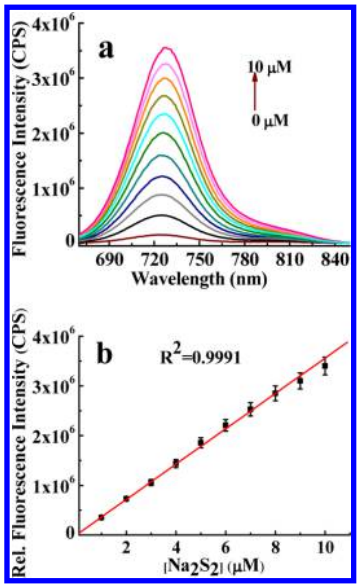

Figure 2. Fluorescence spectra of Mito-ss (10 μM) upon addition of Na_2S_2 (0−10 μM) (a) and the corresponding linear relationship between the fluorescent intensity and Na_2S_2 concentrations (b). Spectra were acquired in 10 mM HEPES buffer (pH 7.4, 0.5% DMSO, 0.4% Tween 80) after incubation with various concentrations of Na_2S_2 for 5 min at 37 °C. λ_{ex} = 675 nm, λ_{em} = 730 nm.

increasing concentrations of Na_2S_2, the fluorescence intensity of Mito-ss gradually increased with a center at 730 nm which located in the NIR region. Additionally, the absorption spectra were also examined under simulated physiological conditions. UV−vis spectra of Mito-ss exhibited absorption band at 660 nm. After treated Mito-ss with Na_2S_2, a new absorption peak appeared at 688 nm, which was the typical absorption of azo-BODIPY fluorophore. Simultaneously, an isosbestic point was formed at 675 nm (Supporting Information Figure S4). Figure 2b displayed a linear correlation between various concentrations of Na_2S_2 and observed fluorescence intensities at 730 nm. The regression equation was $F_{\lambda ex/em(675/730\ nm)} = 3.32 \times 10^5 [H_2S_2] + 4.59 \times 10^3$ with a >3-log linear dynamic range, R^2 = 0.9991. The detection limit was determined to be 25 nM ($3\sigma/\kappa$) under the experimental conditions. These results demonstrate that our probe Mito-ss can detect H_2S_n both qualitatively and quantitatively under simulated physiological conditions potentially.

Selectivity to H_2S_n. To evaluate the specificity of Mito-ss for H_2S_n, we then assessed the fluorescence responses of Mito-ss toward other RSS, most of which were biologically related. The concentrations of other RSS (e.g., Cys) and reductive species (e.g., ascorbic acid) are much higher than the average levels of these RSS and reductive species in cells (Table S1 in the Supporting Information). As shown in Figure 3, only H_2S_n (at 10 μM) elicited a dramatic increase in the fluorescence intensity of Mito-ss. Some other RSS, such as Cys, Hcy, GSH, CysSSCys, GSSG, NaHS, Cys-poly sulfide, S_8, $S_2O_3^{2-}$, and

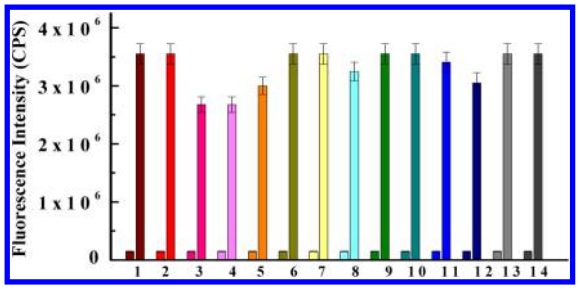

Figure 3. Fluorescence responses of Mito-ss (10 μM) to biologically relevant RSS. In each group, the bars represent relative responses at 730 nm of Mito-ss to RSS and the mixture of RSS with 10 μM Na_2S_2, respectively. Legend: (1) blank +10 μM Na_2S_2; (2) blank +10 μM Na_2S_4; (3) 1 mM Cys + Na_2S_2; (4) 1 mM Hcy + Na_2S_2; (5) 10 mM GSH + Na_2S_2; (6) 1 mM CysSSCys + Na_2S_2; (7) 1 mM GSSG + Na_2S_2; (8) 0.5 mM NaHS + Na_2S_2; (9)1 mM Cys-poly sulfide + Na_2S_2; (10) 0.5 mM S_8 + Na_2S_2; (11) 0.5 mM $Na_2S_2O_3$ + Na_2S_2; (12) 0.5 mM $NaHSO_3$ + Na_2S_2; (13) 1 mM ascorbic acid + Na_2S_2; (14) 1 mM tocopherol + Na_2S_2. Data were recorded in 10 mM HEPES buffer (pH 7.4, 0.5% DMSO and 0.4% Tween 80) at 37 °C for 35 min. λ_{ex} = 675 nm and λ_{em} = 730 nm.

HSO_3^-, did not trigger any fluorescence enhancement. In addition, Mito-ss was also considerably inert to other reductive species such as ascorbic acid and tocopherol. As the probe showed high selectivity toward H_2S_n, we also performed the competition experiments in the presence of Na_2S_2. Exposing Mito-ss to a mixture of RSS and Na_2S_2 almost yielded the same fluorescence enhancement as that only treated with Na_2S_2. Among them, Cys, Hcy, GSH, and $NaHSO_3$ caused a little interference in the fluorecense response, presumably due to H_2S_2 could react with biothiols, resulting in the consumption of H_2S_2 in solutions.[38] These results demonstrate that our probe can be used for the selective detection of H_2S_n in the presence of a high concentration of biological thiols.

Sources of H_2S_n. H_2S_n may be generated by their own biosynthetic pathways, until now it remains unclear. Recent studies suggest H_2S_n can derive from H_2S in the presence of reactive oxygen species (ROS).[39,40] We then utilized Mito-ss to detect H_2S_n generated from the reaction of H_2S and ROS. As shown in Figure 4, Mito-ss displayed weak fluorescence responses to ROS and reactive nitrogen species (RNS),

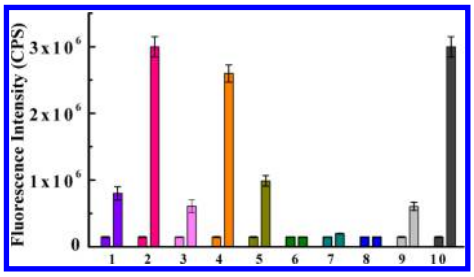

Figure 4. Fluorescence responses of Mito-ss (10 μM) to various ROS and RNS in the presence of H_2S or GPx. In each group, the bars represent relative responses of Mito-ss to ROS/RNS and the mixture of ROS/RNS with NaHS (50 μM) or GPx (500U/L), respectively. Legend: (1) 50 μM H_2O_2 + NaHS; (2) 50 μM H_2O_2 + NaHS + GPx; (3) 50 μM $O_2^{\bullet-}$ + NaHS; (4) 50 μM $O_2^{\bullet-}$ + NaHS+ GPx; (5) 50 μM $^{\bullet}OH$ + NaHS; (6) 50 μM MeLOOH + NaHS; (7) 50 μM *t*-BuOOH + NaHS; (8) 50 μM NO + NaHS; (9) 50 μM $ONOO^-$ + NaHS; (10) 50 μM ClO^- + NaHS. Data were acquired in 10 mM HEPES buffer (pH 7.4, 0.5% DMSO and 0.4% Tween 80) at 37 °C for 35 min. λ_{ex} = 675 nm and λ_{em} = 730 nm.

DOI: 10.1021/ac5044237
Anal. Chem. 2015, 87, 3631−3638

whereas significant fluorescence intensities were obtained upon further addition of NaHS, which indicated that H_2S_n was formed. Especially, ClO^- and H_2S elicited the strongest intensity, which illustrated that ClO^- was the most effective ROS utilizing H_2S to produce H_2S_n. In contrast, Mito-ss was inert to the MeLOOH, *t*-BuOOH, NO, which exhibit little fluorescence intensity changes after added NaHS. Obviously, we found that the chemical synthetic pathway of H_2S_n was slowly so that inconsistent with the rapid metabolism of endogenous H_2S_n in biological systems. It is reported that glutathione peroxidase (GPx) can scavenge ROS through converting H_2S to H_2S_n.[41] Next, to accelerate the reaction rate of H_2S_n formation, GPx was added as a catalyst. As expected, within 15 min, a remarkable change in the fluorescence intensity was obtained (group 2 and group 4 in Figure 4). Therefore, GPx could be participated in the reaction between ROS and H_2S as catalyst. All together, these results demonstrate that our probe is suitable for detecting H_2S_n generated from H_2S and ROS.

Although H_2S_n has been proposed to be produced between H_2S and ROS, it is found that hydrogen polysulfide-derivatives can be also synthesized from cystine by cystathionine γ-lyase (CSE).[9−11,42] Since there exists a dynamic distribution among hydrogen polysulfide species,[12−16] we then evaluated the roles of the enzyme CSE in hydrogen polysulfides generation. Another enzyme cystathionine β-synthase (CBS) was also tested. As shown in Figure 5, both the enzymes CSE and CBS

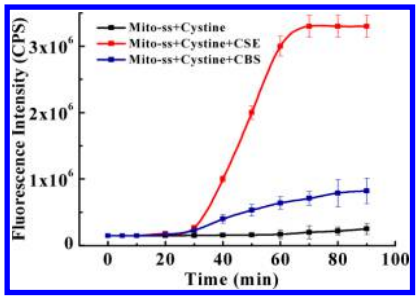

Figure 5. Fluorescence responses of Mito-ss (10 μM) toward hydrogen polysulfides catalyzed by CSE (50 μg/mL) and CBS (5 μg/mL) using cystine (1.25 mM) as a substrate. Data were acquired in 10 mM HEPES buffer (pH 7.4, 0.5% DMSO and 0.4% Tween 80) containing 50 μM pyridoxial phosphate at 37 °C for 35 min. λ_{ex} = 675 nm, λ_{em} = 730 nm.

could induce the fluorescence intensity changes, which indicated that the enzymes CSE and CBS could directly generate H_2S_n when used cystine as substrate. However, the fluorescence response to CSE was stronger than that of CBS. We attributed the phenomenon to the origin different physiological functions of the two enzymes. The reaction of enzyme CSE with cystine were mainly gererated hydrogen polysulfide species, while the enzyme CBS predominantly produced polysulfides first and then converted to hydrogen polysulfides in the presence of cysteine and glutathione.[9−11] Taken together, all these results confirm that our probe can be used to detect enzymatic H_2S_n in biochemical systems.

Imaging H_2S_n in Cells. Overall, the above results suggest that our new fluorescent probe holds great potential applications in complicated biological systems. Then, we chose the mouse macrophage cell line RAW264.7 as a bioassay model. Mito-ss was then tested for its ability to respond to H_2S_n in RAW264.7 cells. First, RAW264.7 cells were incubated with Mito-ss (1 μM) for 15 min at 37 °C as control showed faint fluorescence (Figure 6a). However, after the same treatment

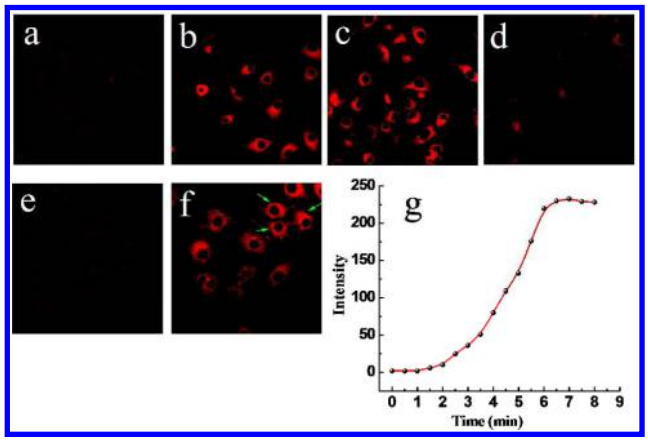

Figure 6. Confocal microscopy images of live RAW264.7 cells visualizing H_2S_n level changes using Mito-ss (1 μM). Images displayed represent emission intensities collected in optical windows between 700 and 800 nm upon excitation at 635 nm for Mito-ss. (a) RAW264.7 cells incubated with Mito-ss for 15 min at 37 °C. (b) RAW264.7 cells preincubated with Mito-ss for 15 min and washed with DMEM. The cells further incubated with Na_2S_2 (1 μM) for 15 min at 37 °C. (c) RAW264.7 cells preincubated with 1 μg/mL LPS for 16 h at 37 °C and incubated with Mito-ss for 15 min. (d) RAW264.7 cells preincubated with PAG (100 μM) for 10 min and further addition with 1 μg/mL LPS for 16 h at 37 °C. Then the cells incubated with Mito-ss for 15 min. (e) RAW264.7 cells preincubated with 2.5 ng/mL PMA for 30 min at 37 °C and incubated with Mito-ss for 15 min. (f) After the same treatment with (e), the cells were washed with DMEM, then the cells were incubated with NaHS for 15 min at 37 °C. (g)The real-time fluorescence enhancements of the selected cells in figure (f).

with the control, the cells were washed with Dulbecco's Modified Eagle Medium (DMEM) to remove the excess Mito-ss and further treated with Na_2S_2 for another 15 min. As expected, strong fluorescence in the cells was observed (Figure 6b). Another cells which treated with NaHS gave little fluorescence response (Supporting Information Figure S6). These results demonstrate that Mito-ss can be employed to directly detect H_2S_n added exogenously in living cells.

Having got our probe could image supplemented H_2S_n exogenously, we sought to determine whether our probe could detect endogenous produced H_2S_n by perturbing the pool of H_2S_n in RAW264.7 cells. Lipopolysaccharide (LPS, 1 μg/mL) can induce CSE mRNA overexpression for promoting the initial real-time production rate of H_2S_n.[10,43] Thus, RAW264.7 cells were first stimulated by LPS for 16 h to monitor H_2S_n produced endogenously and then incubated with Mito-ss for 15 min. Obviously, the cells displayed a dramatic increase in intracellular fluorescence intensity (Figure 6c). Next, we performed an additional control experiment, the cells were pretreated with a CSE inhibitor, DL-propargylglycine[44] (PAG, 100 μM) for 10 min and stimulated with LPS for 16 h. Subsequently, the cells were incubated with Mito-ss for another 15 min. As expected, the fluorescence response was attenuated, indicating that CSE contribute to the observed H_2S_n generation (Figure 6d). All these data further indicate that our probe enables direct visualization of endogenous H_2S_n changes in living cells.

We have confirmed that H_2S_n can be formed when H_2S encounters intracellular oxidants (Figure 4), such as H_2O_2,

DOI: 10.1021/ac5044237
Anal. Chem. 2015, 87, 3631−3638

superoxide, and hypochlorous acid (HOCl).[39,40] After building on the characterization studies of H_2S_n synthesis under the simulated physiological conditions, we next turned our attention to imaging H_2S_n, which produced from ROS and H_2S in RAW264.7 cells. The cells were first stimulated with phorbol 12-myristate 13-acetate (PMA, 2.5 ng/mL) for 30 min to provide an overproduction of ROS,[45,46] then incubated with Mito-ss (1 μM) for 15 min. Subsequently, the cells were washed with DMEM to remove the excess Mito-ss, and further treated with NaHS for 15 min. As expected, strong fluorescence was induced in these cells, which provided a clear demonstration that ROS could react with H_2S to form H_2S_n in RAW264.7 cells (Figure 6f). Additionally, the mean fluorescence intensity changes of the cells over time in Figure 6f (labeled with green arrow) were recorded to allow for direct comparisons (Figure 6g). Within only 6 min, the reaction had reached saturation, which attributed to the catalysis of GPx. Because RAW264.7 cells employ GPx to regulate antioxidants and anti-inflammatory activities.[47] As a control, the cells not treated with NaHS were also imaged. Clearly, no fluorescence response was observed (Figure 6e). Taken together, these results indicate that Mito-ss can indeed be used in the detection of H_2S_n produced from ROS and H_2S in RAW264.7 cells.

We next investigate whether our probe can function well in different kinds of living cells which may express varied endogenous H_2S_n. We performed the tests by employing other five cell lines: human astrocytoma (U87) cells, human umbilical vein endothelial cells (HUVECs), human lung carcinoma (A549) cells, Hela cells, and human hepatocellular liver carcinoma (HepG2) cells. As displayed in Figure 7, Mito-ss could respond to H_2S_n level changes in different cell lines. To further confirm our probe could detect the endogenous H_2S_n changes in cells, the CSE were overexpressed in A549 cells to dramatically increase the concentration of H_2S_n (Figure 7d right plate). As shown in Figure 7d (right plate), the probe Mito-ss was sensitive enough to detect the endogenous H_2S_n changes in living cells. To further confirm the fluorescence changes in living cells, we carried out flow cytometry assay to test and verify the results in Figure 7. As shown in Supporting Information Figure S12, the results were consistent with the results in Figure 7. The results demonstrate that our probe Mito-ss can detect H_2S_n in different kinds of living cells.

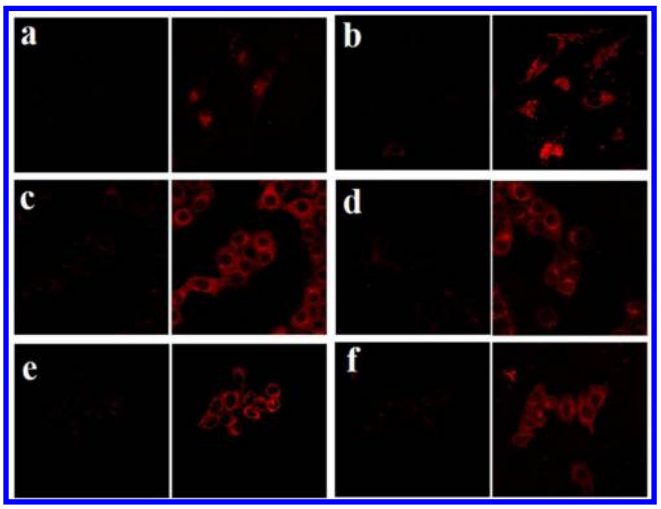

Figure 7. Confocal microscopy images of live cells for visualizing H_2S_n level changes using Mito-ss (1 μM). Group a: Human astrocytoma (U87) cells. Group b: Human umbilical vein endothelial cells (HUVECs). Group c: Human lung carcinoma (A549) cells. Group d: A549 cells (with overexpression of CSE or not). Group e: Hela cells. Group f: Human hepatocellular liver carcinoma (HepG2) cells. The cells in each group: the left cells were controls, and the right cells were incubated with Na_2S_2 (1 μM) for 15 min at 37 °C. All cells preincubated with Mito-ss for 15 min and washed with DMEM. Images displayed represent emission intensities collected in optical windows between 700 and 800 nm upon excitation at 635 nm for Mito-ss.

Sublocation in Cells. Mitochondria are the powerhouse of cells, which involved in signaling, cellular differentiation, cell death, as well as the control of the cell cycle and cell growth.[48] In addition, mitochondria are the main production source of ROS. Once the ROS produced excessively, the oxidative stress is caused and leading to cell injury and death, which contribute to many diseases such as aging, cancer, neurodegenerative and cardiovascular diseases.[49−52] Fortunately, the mitochondria fraction contains approximately 60% of bound sulfane sulfur, which involves H_2S_n that exhibit antioxidant and cytoprotective properties.[8] Thus, H_2S_n may play protective effects on the cells against the damage caused by oxidative stress and maintain cellular redox homeostasis in the antioxidant defense systems. In this work, Mito-ss exhibits a significant ability to target mitochondria because of the lipophilic triphenylphosphonium cation.[53] Next, we tested whether Mito-ss could monitor the mitochondrial H_2S_n level changes in live cells. Endogenous H_2S_n were produced via stimulating RAW264.7 cells by LPS for 16 h. After washing with DMEM, the cells were then stained with Hoechst 33342 (a commercial nuclear dye) for 30 min, rhodamine 123 (a commercial mitochondria marker) and Mito-ss for 15 min. Employing the Image-Pro Plus software, we obtained the spectrally separated images acquired from the three dyes (Figure 8a−c). Moreover, the color−pair intensity correlation analysis of Figure 8a−c were also performed and shown in Figure 8d−f, only the intensity distribution of Mito-ss and rhodamine 123 showed a high correlated plot. The image of Mito-ss merged well with the image of the rhodamine 123, thereby implying a preferential distribution of Mito-ss in mitochondria (Figure 8g, the cells were selected in Figure 8a). The intensity profiles of the linear regions of interest across RAW264.7 cells costained with Mito-ss and rhodamine 123 (red arrow in Figure 8g) were varying in close synchrony (Figure 8h). In addition, the Pearson's colocalization coefficient of the Mito-ss and rhodamine 123 was Rr = 0.97, while the Manders' coefficients were m_1 = 0.99, m_2 = 0.98. Taken together, this preliminary imaging study convince that Mito-ss can specifically real-time detect the H_2S_n level changes in cellular mitochondria, which is of great importance to clarify the physiological roles of H_2S_n in the organelle. In addition, the MTT assay for Mito-ss was conducted, the result clearly demonstrated that the probe exhibited low cytotoxicity to living cells under experimental conditions (Supporting Information Figure S10).

Imaging H_2S_n in Vivo and in Vitro. Our probe functions in the NIR region that allows for imaging with high tissue penetration, minimal photo damage to biological samples and minimum interference from background autofluorescence in living systems. We further evaluated the suitability of the probe for visualization of H_2S_n in living animals. BALB/c mice were selected and divided into two groups. One group was given an i.p. injection of Mito-ss as control. Twenty minutes later, the other group was given an injection of 10 equiv of Na_2S_2 after the same treatment of the control mice. As shown in Figure 9a,

DOI: 10.1021/ac5044237
Anal. Chem. 2015, 87, 3631−3638

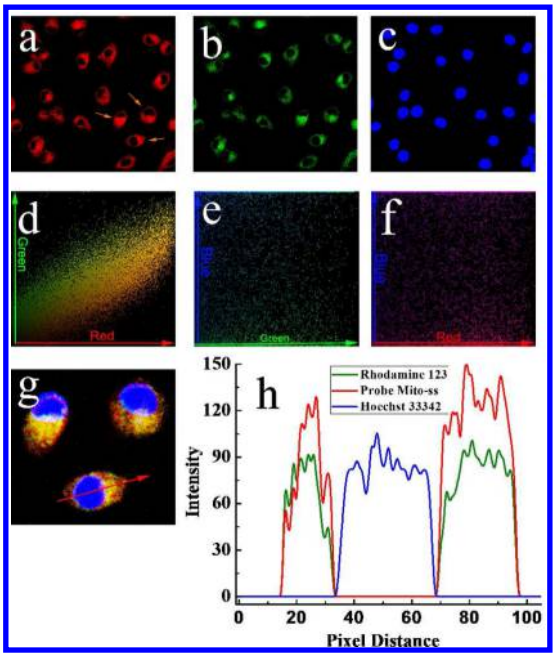

Figure 8. Confocal microscopy images of live RAW264.7 cells costained by Mito-ss (1 μM), rhodamine 123 (1 μg/mL) and Hoechst 33342 (1 μg/mL). RAW264.7 cells treated with LPS (1 μg/mL) for 16 h, then washed with DMEM. The cells then further incubated with Hoechst 33342 for 30 min, rhodamine 123 and Mito-ss for 15 min at 37 °C and imaged with Mito-ss (a), rhodamine 123 (b), and Hoechst 33342 (c). Fluorescence confocal microscopic images constructed from 700 to 800 nm for (a), from 550 to 600 nm for (b) and from 425 to 500 nm for (c) fluorescence collection windows, λ_{ex} = 635, 515, and 405 nm, respectively. (d) Displayed the colocalization areas of the red and green channels selected. (e) Displayed the colocalization areas of the blue and green channels selected. (f) Displayed the colocalization areas of the red and blue channels selected. (g) Enlarged areas of overlay of selected portions of panels a−c. (h) Intensity profile of regions of interest (red arrow in panel g) across RAW264.7 cells.

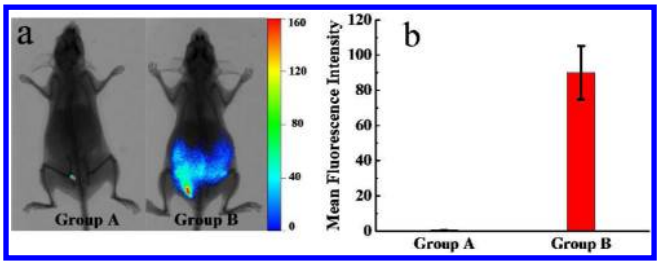

Figure 9. Representative fluorescence images of visualizing H_2S_n levels in mice using Mito-ss. (a) Group A injected i.p. with Mito-ss (10 μM, 50 μL in 1:9 DMSO/saline v/v). Group B injected i.p. with Na_2S_2 (100 μM, 50 μL in saline) after the same treatment with Group A. (b) Quantification of total photon flux from each group. The total number of photons from the entire peritoneal cavity of the mice was integrated. Images were taken after incubation for 30 min. Images were taken from 700 nm fluorescence collection window. λ_{ex} = 670 nm. n = 5. Error bars are ± SEM.

the control group showed almost no fluorescence. The mice injected with Na_2S_2 displayed a strong fluorescence indicating that Mito-ss could respond to Na_2S_2 in mice. In addition, the mean fluorescence intensity of each group was quantified and shown in Figure 9b. The group that injected with Na_2S_2 exhibits 180-fold fluorescence enhancements. Moreover, we applied our probe to the determination of H_2S_n concentrations in serum using the BALB/c mouse model. As shown in Supporting Information Figure S13, the H_2S_n concentration in the serum of mice was 1.57 μM. These experiments establish that our probe is capable of imaging H_2S_n successfully in vivo for the first time.

Since the probe Mito-ss functioned well in cells and in mice, we finally attempted to qualitatively evaluate the concentrations of H_2S_n in ex vivo-dissected organs. The results of fluorescence tests for tissue homogenates (tissue 1 g in 10 mL of saline) reveal that the concentrations of H_2S_n in the brain and kidney are much higher than other organs, including the liver, heart, and lung (Figure 10). The higher concentration of H_2S_n in the

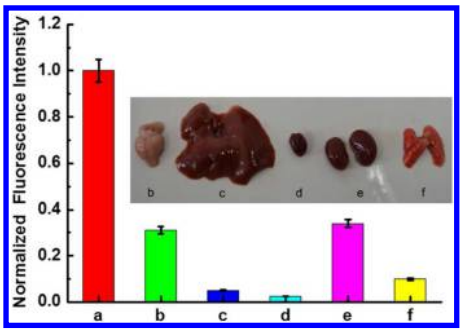

Figure 10. Qualitative evaluation of H_2S_n concentrations in Ex vivo-dissected organs. (a) The fluorescence response to 10 μM Na_2S_2 in 10 mM HEPES buffer with 15% serum for 5 min at 37 °C as control. (b−f) Fluorescence responses to ex vivo-dissected organs: (b) brain, (c) liver, (d) heart, (e) kidney, and (f) lung. The fluorescent intensities were presented with normalized. λ_{ex} = 675 nm and λ_{em} = 730 nm. n = 5. Error bars are ± SEM.

brain is consistent with the high H_2S concentration which is determined to be 5.0 ± 2.0 μmol g^{-1} protein.[54] The brain tissue often consumes large amounts of oxygen. The high dose of cerebral oxygen consumption may benefit for the redox chemistry between H_2S_n and H_2S. The fact that the kidney expresses the highest levels of the H_2S-forming enzyme CSE[55] may make a high level of H_2S_n existing in kidney. Although the liver contains high level of biothiols (mainly are GSH and Cys),[56] the result of our probe indicates that the concentration of H_2S_n in liver may be relatively low. These results display that the probe Mito-ss can be applied to access the concentrations of H_2S_n in ex vivo-dissected organs.

■ CONCLUSIONS

In summary, we present a fluorescent probe Mito-ss for evaluating H_2S_n in cells as well as in vivo. Mito-ss employs nitro-activated fluorobenzoiate for H_2S_n trapping and utilizes the lipophilic triphenylphosphonium cation to sublocate in mitochondria. This mitochondria-targeted fluorescent probe shows high selective turn-on fluorescence response to H_2S_n over a variety of RSS, RNS, and ROS. We verify that H_2S_n can be derived from H_2S in the presence of ROS catalyzed by GPx. And the enzymes CSE and CBS are proven to contribute to the direct generation of H_2S_n. Mito-ss behaves a promising fluorescent probe for monitoring H_2S_n production in cells, no matter which supplement methods adopt, exogenously added or produced via enzymatic activity. The probe is also successfully utilized to visualization of H_2S_n in mice. In short, Mito-ss can be utilized to study the roles of H_2S_n in physiological and pathological processes, which may help to

DOI: 10.1021/ac5044237
Anal. Chem. 2015, 87, 3631−3638

elucidate H_2S_n biosynthetic pathways and uncover new mechanism responsible for H_2S_n homeostasis.

■ ASSOCIATED CONTENT

Supporting Information

Experimental supplementary methods for chemical synthesis and characterization of compounds, supplementary experiments, and data. This material is available free of charge via the Internet at http://pubs.acs.org.

■ AUTHOR INFORMATION

Corresponding Author

*E-mail: lxchen@yic.ac.cn.

Author Contributions

M.G. and F.Y. contributed equally.

Notes

The authors declare no competing financial interest.

■ ACKNOWLEDGMENTS

We thank National Nature Science Foundation of China (NSFC) (NO.21405172, No.21275158), the Innovation Projects of the CAS (Grant KZCX2-EW-206), and the program of Youth Innovation Promotion Association, CAS (Grant 2015170).

■ REFERENCES

(1) Giles, G.; Tasker, K. M.; Jacob, C. *Free Radical Biol. Med.* **2001**, *31*, 1279−1283.
(2) Tangerman, A. *J. Chromatogr. B: Anal. Technol. Biomed. Life Sci.* **2009**, *877*, 3366−3377.
(3) Nagy, P.; Ashby, M. T. *J. Am. Chem. Soc.* **2007**, *129*, 14082−14091.
(4) Bindoli, A.; Fukuto, J. M.; Forman, H. J. *Antioxid. Redox Signal.* **2008**, *10*, 1549−1564.
(5) Paul, B. D.; Snyder, S. H. *Nat. Rev. Mol. Cell. Biol.* **2012**, *13*, 499−507.
(6) Yu, F.; Han, X.; Chen, L. *Chem. Commun.* **2014**, *50*, 12234−12249.
(7) Lin, V. S.; Chang, C. J. *Curr. Opin. Chem. Biol.* **2012**, *16*, 595−601.
(8) Jackson, M. R.; Melideo, S. L.; Jorns, M. S. *Biochemistry* **2012**, *51*, 6804−6815.
(9) Iciek, M.; Wlodek, L. *Polym. J. Pharmcol.* **2001**, *53*, 215−225.
(10) Ida, T.; Sawa, T.; Ihara, H.; Tsuchiya, Y.; Watanabe, Y.; Kumagai, Y.; Suematsu, M.; Motohashi, H.; Fujii, S.; Matsunaga, T.; Yamamoto, M.; Ono, K.; Devarie-Baez, N. O.; Xian, M.; J. Fukuto, M.; Akaike, T. *Proc. Natl. Acad. Sci. U. S. A.* **2014**, *111*, 7606−7611.
(11) Bailey, T. S.; Zakharov, L. N.; Pluth, M. D. *J. Am. Chem. Soc.* **2014**, *136*, 10573−10576.
(12) Nagy, P.; Pálinkás, Z.; Nagy, A.; Budai, B.; Tóth, I.; Vasas, A. *Biochim. Biophys. Acta* **2014**, *1840*, 876−891.
(13) Kimura, H. *Neurochem. Int.* **2013**, *63*, 492−497.
(14) Kabil, O.; Motl, N.; Banerjee, R. *Biochim. Biophys. Acta* **2014**, *1844*, 1355−1366.
(15) Koike, S.; Ogasawara, Y.; Shibuya, N.; Kimura, H.; Ishii, K. *FEBS Lett.* **2013**, *587*, 3548−3555.
(16) Kimura, Y.; Mikami, Y.; Osumi, K.; Tsugane, M.; Oka, J.; Kimura, H. *FASEB J.* **2013**, *27*, 2451−2457.
(17) Greiner, R.; Pálinkás, Z.; Bäsell, K.; Becher, D.; Antelmann, H.; Nagy, P.; Dick, T. P. *Antioxid. Redox Signal.* **2013**, *19*, 1749−1765.
(18) Liu, C.; Pan, J.; Li, S.; Zhao, Y.; Wu, L.; Berkman, C. E.; Whorton, A. R.; Xian, M. *Angew. Chem., Int. Ed.* **2011**, *50*, 10327−10329.
(19) Mao, G. J.; Wei, T. T.; Wang, X. X.; Huan, S. Y.; Lu, D. Q.; Zhang, J.; Zhang, X. B.; Tan, W.; Shen, G. L.; Yu, R. Q. *Anal. Chem.* **2013**, *85*, 7875−7881.
(20) Chen, X.; Zhou, Y.; Peng, X.; Yoon, J. *Chem. Soc. Rev.* **2010**, *39*, 2120−2135.
(21) Li, X.; Gao, X.; Shi, W.; Ma, H. *Chem. Rev.* **2014**, *114*, 590−659.
(22) Paulsen, C. E.; Carroll, K. S. *Chem. Rev.* **2013**, *113*, 4633−4679.
(23) Yang, Y.; Zhao, Q.; Feng, W.; Li, F. *Chem. Rev.* **2013**, *113*, 192−270.
(24) Yuan, L.; Lin, W.; Zheng, K.; He, L.; Huang, W. *Chem. Soc. Rev.* **2012**, *42*, 622−661.
(25) Fan, J.; Hu, M.; Zhan, P.; Peng, X. *Chem. Soc. Rev.* **2013**, *42*, 29−43.
(26) Chan, J.; Dodani, S. C.; Chang, C. J. *Nat. Chem.* **2012**, *4*, 973−984.
(27) Guo, Z.; Nam, S.; Park, S.; Yoon, J. *Chem. Sci.* **2012**, *3*, 2760−2765.
(28) Ozawa, T.; Yoshimura, H.; Kim, S. B. *Anal. Chem.* **2013**, *85*, 590−609.
(29) Sun, M.; Yu, H.; Zhu, H.; Ma, F.; Zhang, S.; Huang, D.; Wang, S. *Anal. Chem.* **2014**, *86*, 671−677.
(30) Yang, S.; Qi, Y.; Liu, C.; Wang, Y.; Zhao, Y.; Wang, L.; Li, J.; Tan, W.; Yang, R. *Anal. Chem.* **2014**, *86*, 7508−7515.
(31) Liu, C.; Chen, W.; Shi, W.; Peng, B.; Zhao, Y.; Ma, H.; Xian, M. *J. Am. Chem. Soc.* **2014**, *136*, 7257−7260.
(32) Chen, W.; Liu, C.; Peng, B.; Zhao, Y.; Pacheco, A.; Xian, M. *Chem. Sci.* **2013**, *4*, 2892−2896.
(33) Shi, W. J.; EI-Khouly, M. E.; Ohkubo, K.; Fukuzumi, S.; Nq, D. K. *Chemistry.* **2013**, *19*, 11332−11349.
(34) Bhuniya, S.; Lee, M. H.; Jeon, H. M.; Han, J. H.; Lee, J. H.; Park, N.; Maiti, S.; Kang, C.; Kim, J. S. *Chem. Commun.* **2013**, *49*, 7141−7143.
(35) Wang, R.; Chen, L.; Liu, P.; Wang, Q.; Wang, Y. *Chemistry* **2012**, *18*, 11343−11349.
(36) Wang, R.; Yu, F.; Chen, L.; Chen, H.; Wang, L.; Zhang, W. *Chem. Commun.* **2012**, *48*, 11757−11759.
(37) Yu, F.; Li, P.; Li, G.; Zhao, G.; Chu, T.; Han, K. *J. Am. Chem. Soc.* **2011**, *133*, 11030−11033.
(38) Toohey, J. I. *Biochem. J.* **1989**, *264*, 625−632.
(39) Nagy, P.; Winterbourn, C. C. *Chem. Res. Toxicol.* **2010**, *23*, 1541−1543.
(40) Predmore, B. L.; Lefer, D. J.; Gojon, G. *Antioxid. Redox Signal.* **2012**, *17*, 119−140.
(41) Winterbourn, C. C. *Nat. Chem. Biol.* **2008**, *4*, 278−286.
(42) Francoleon, N. E.; Carrington, S. J.; Fukuto, J. M. *Arch. Biochem. Biophys.* **2011**, *516*, 146−153.
(43) Zhu, X.; Liu, S.; Liu, Y.; Wang, S.; Ni, X. *Cell. Mol. Life Sci.* **2010**, *67*, 1119−1132.
(44) Lin, V. S.; Lippert, A. R.; Chang, C. J. *Proc. Natl. Acad. Sci. U. S. A.* **2013**, *110*, 7131−7135.
(45) Pu, K.; Shuhendler, A. J.; Rao, J. *Angew. Chem., Int. Ed.* **2013**, *52*, 10325−10329.
(46) Hecker, E.; Schmidt, R. *Fortschr. Chem. Org. Naturst.* **1974**, *31*, 377−467.
(47) Jung, W. J.; Sung, M. K. *Biofactors* **2004**, *21*, 113−117.
(48) Green, D. R.; Galluzzi, L.; Kroemer, G. *Science* **2011**, *333*, 1109−1112.
(49) Finkel, T.; Serrano, M.; Blasco, M. A. *Nature* **2007**, *448*, 767−774.
(50) Wang, Y. Y.; Chen, S. M.; Li, H. *Acta Pharmacol. Sin.* **2010**, *31*, 160−164.
(51) Yu, H.; Zhang, X.; Xiao, Y.; Zou, W.; Wang, L.; Jin, L. *Anal. Chem.* **2013**, *85*, 7076−7084.
(52) Li, P.; Zhang, W.; Li, K.; Liu, X.; Xiao, H.; Zhang, W.; Tang, B. *Anal. Chem.* **2013**, *85*, 9877−9881.
(53) Ross, M. F.; Kelso, G. F.; Blaikie, F. H.; James, A. M.; Cochemé, H. M.; Filipovska, A.; Da Ros, T.; Hurd, T. R.; Smith, R. A.; Murphy, M. P. *Biochemistry (Moscow)* **2005**, *70*, 222−230.
(54) Qian, Y.; Zhang, L.; Ding, S.; Deng, X.; He, C.; Zheng, X. E.; Zhu, H. L.; Zhao, J. *Chem. Sci.* **2012**, *3*, 2920−2923.
(55) Wagner, C. A. *J. Nephrol.* **2009**, *22*, 173−176.
(56) Kamoun, P. *Amino Acids* **2004**, *26*, 243−254.

DOI: 10.1021/ac5044237
Anal. Chem. 2015, 87, 3631−3638